BRIEF COMMUNICATIONS

Calbindin controls release probability in ventral tegmental area dopamine neurons

Ping-Yue Pan & Timothy A Ryan

Relatively little is known about the molecular control of midbrain dopamine release. Using high-fidelity imaging of pHluorin-tagged vesicular monoamine transporter 2 in dopamine neurons, we found that exocytosis was more loosely coupled to calcium entry than in fast synapses. In ventral tegmental area neurons, this allows exocytosis to be efficiently controlled by a native fast calcium buffer, calbindin-D28k, maintaining a lower vesicular release probability compared with substantia nigra neurons.

The human brain contains only ~600,000 dopamine (DA) neurons, and a large fraction of these originate in the midbrain substantia nigra pars compacta (SN, nucleus A9) and ventral tegmental area (VTA, nucleus A10), which respectively modify neuronal circuit function in the basal ganglia and the meso-cortical and meso-limbic pathways. Despite the clinical relevance of dopaminergic modulation[1–3], relatively little is known about the molecular control of dopamine release itself, especially the potential difference and molecular determinants in dopamine release characteristics between VTA and SN neurons. One unique feature of dopaminergic transmission is that it is mediated by slow G protein–coupled receptor–mediated signaling. We used an optical assay employing pHluorin, a variant of GFP whose fluorescence is quenched by protonation with a $pK_a = 7.1$ (refs. 4,5), to measure exocytosis in DA neurons.

pHluorin-tagged vesicular monoamine transporter 2 (vMAT-pHluorin)[6] displays low surface fractions ($6.2 \pm 2.1\%$, $N = 7$) when expressed in midbrain DA neurons, permitting measurements of single action potential responses (**Fig. 1a**) at fast time resolution. The size of the exocytic response is a reflection of the size of the readily releasable pool (RRP) and the probability that a vesicle in the RRP will undergo exocytosis following action potential stimulation (P_v; **Supplementary Fig. 1**). P_v is, in turn, determined by the likelihood that the calcium sensor for exocytosis will bind sufficient Ca^{2+} to trigger exocytosis. The relative coupling of calcium channels and sites of exocytosis is therefore a key determinant of P_v. In DA nerve terminals, application of EGTA-AM that resulted in a ~55% drop in measured action potential–triggered Ca^{2+} signal led to a 65% drop in exocytosis, whereas, in more conventional fast hippocampal terminals, a similar reduction in Ca^{2+} signal led to a more modest (~35%) drop in exocytosis (**Fig. 1**). Thus, exocytosis in DA terminals is more loosely coupled to calcium influx than in hippocampal neurons.

VTA DA neurons are known to be enriched compared with SN neurons in the fastest-known (k_{on} ~8.0×10^7 M^{-1} s^{-1}) endogenous calcium buffering protein, calbindin-D28k[7–9]. In dissociated DA neurons derived from VTA and SN (mixed culture), we found that calbindin-D28k immunoreactivity varied over a 300-fold range (**Fig. 2a,b**), whereas DA neurons extracted from more restricted VTA-enriched midbrain dissections (**Fig. 2c**) showed a significant enrichment in calbindin-D28k ($P = 0.007$, Kolmogorov-Smirnov test; **Fig. 2d**). In contrast, at synapses formed between dissociated hippocampal neurons, calbindin-D28k expression was ~85% lower than in VTA DA neurons (**Supplementary Fig. 2**).

Figure 1 Synaptic vesicles are loosely coupled to calcium entry in DA neurons. (**a**) Difference (ΔF) images of vMAT-pHluorin responses in DA neuron boutons to a single action potential stimulus (left) and NH_4Cl perfusion (right). Scale bar represents 5 μm. (**b**) Average vMAT-pHluorin and vGlut-pHluorin responses to a single action potential stimuli before and after EGTA-AM treatment ($n = 4$ trials). Scale bar represents 400 ms. HP, hippocampal. (**c**) Single action potential ΔF Fluo5F responses of VAMP-mCherry–expressing DA and hippocampal boutons and their corresponding kinetics before and after EGTA-AM treatment. Scale bar represents 400 ms (top panel) and 100 ms (lower panels). (**d**) EGTA treatment preferentially suppressed pHluorin responses in DA terminals ($68 \pm 6\%$) compared with hippocampal terminals ($38 \pm 5\%$) (**$P = 0.004$) for similar suppression of calcium signals (*$P = 0.74$; $56 \pm 6\%$ suppression in DA terminals, $54 \pm 4\%$ suppression in hippocampal terminals). Error bars represent s.e.m.
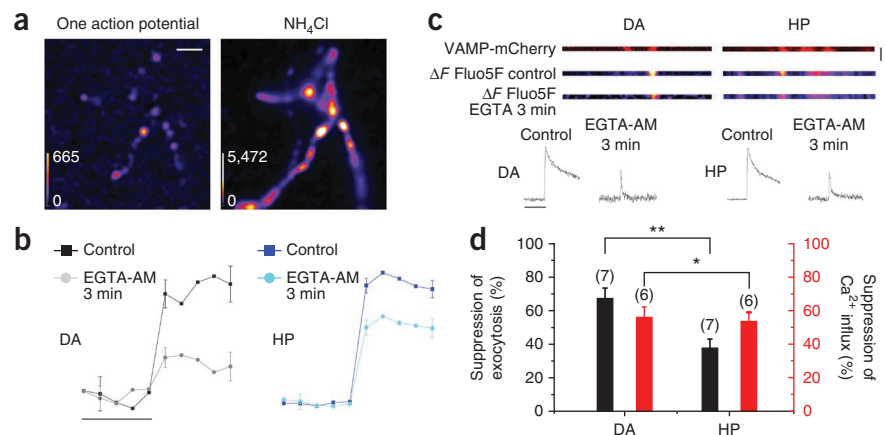
Department of Biochemistry, Weill Cornell Medical College, New York, New York, USA. Correspondence should be addressed to T.A.R. (taryan@med.cornell.edu).
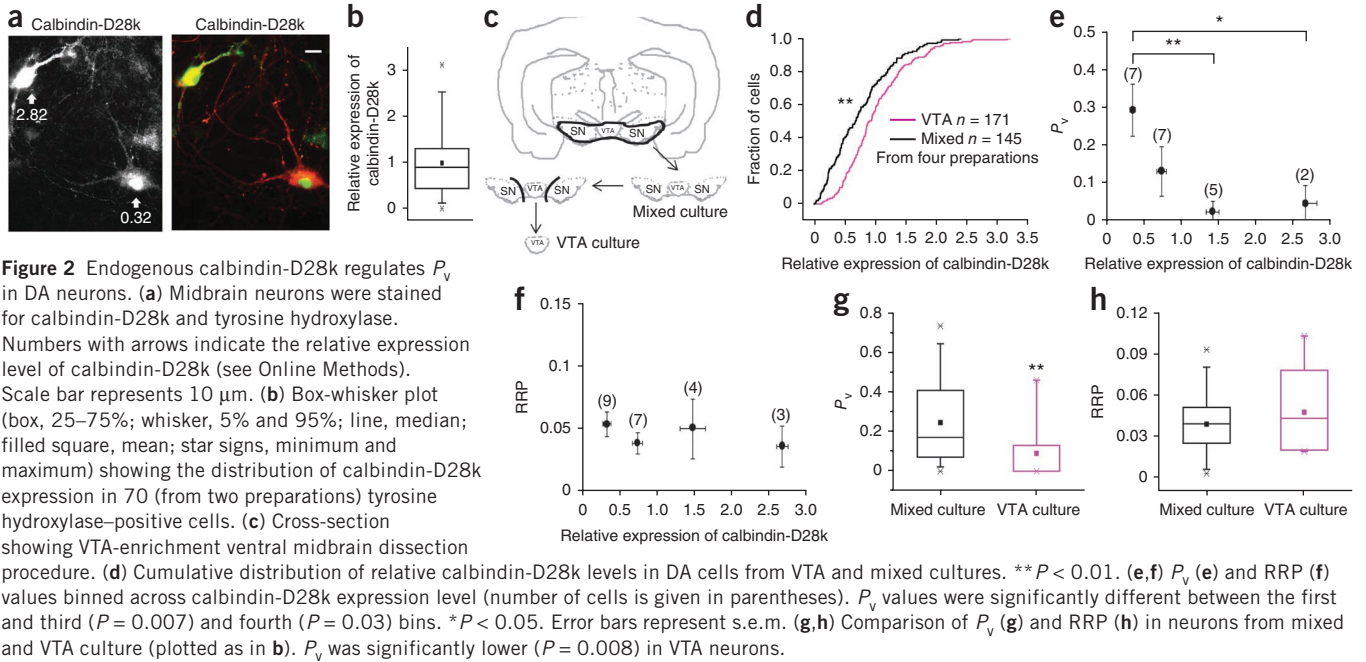
Figure 2 Endogenous calbindin-D28k regulates P_v in DA neurons. (**a**) Midbrain neurons were stained for calbindin-D28k and tyrosine hydroxylase. Numbers with arrows indicate the relative expression level of calbindin-D28k (see Online Methods). Scale bar represents 10 µm. (**b**) Box-whisker plot (box, 25–75%; whisker, 5% and 95%; line, median; filled square, mean; star signs, minimum and maximum) showing the distribution of calbindin-D28k expression in 70 (from two preparations) tyrosine hydroxylase–positive cells. (**c**) Cross-section showing VTA-enrichment ventral midbrain dissection procedure. (**d**) Cumulative distribution of relative calbindin-D28k levels in DA cells from VTA and mixed cultures. **$P < 0.01$. (**e,f**) P_v (**e**) and RRP (**f**) values binned across calbindin-D28k expression level (number of cells is given in parentheses). P_v values were significantly different between the first and third ($P = 0.007$) and fourth ($P = 0.03$) bins. *$P < 0.05$. Error bars represent s.e.m. (**g,h**) Comparison of P_v (**g**) and RRP (**h**) in neurons from mixed and VTA culture (plotted as in **b**). P_v was significantly lower ($P = 0.008$) in VTA neurons.

We previously developed protocols to estimate the size of the RRP (expressed as a fraction of the total recycling pool) and P_v using pHluorin-tagged synaptic vesicle proteins[10]. We used vMAT-pHluorin and these approaches to measure RRP sizes and P_v in DA neurons (**Supplementary Figs. 1** and **3**). We found that P_v and RRP were highly variable across DA cells with mean values of 0.25 ± 0.04 (ranging from 0 ± 0.02 to 0.73 ± 0.01) and 0.039 ± 0.04 (ranging from 0.003 ± 0.002 to 0.083 ± 0.01; **Supplementary Fig. 1**), respectively. Retrospective calbindin-D28k immunocytochemistry for each cell in which these parameters were determined revealed a strong inverse correlation between calbindin-D28k abundance and P_v (**Fig. 2e**), but no correlation with RRP (**Fig. 2f**). DA neurons with the lowest calbindin-D28k levels had an average P_v of 0.30 ± 0.07 and those with the highest calbindin-D28k levels had a P_v of 0.05 ± 0.05 ($P = 0.03$).

Similarly, P_v values were, on average, significantly lower in VTA-enriched DA neurons preparations ($P_v = 0.09 \pm 0.04$) than in VTA and SN cultures ($P_v = 0.25 \pm 0.04$, $P = 0.008$; **Fig. 2g**), whereas RRP sizes were similar (**Fig. 2h**).

To confirm the veracity of the correlation of P_v with calbindin-D28k abundance, we explicitly manipulated calbindin-D28k levels in VTA DA neurons using either knockdown or overexpression (**Supplementary Fig. 4**). In DA neurons expressing a small hairpin RNA (shRNA) targeting calbindin-D28k, expression levels were reduced to 0.13 ± 0.03 of control, whereas neurons transfected with a cDNA encoding full-length rat calbindin-D28k increased expression to 3.16 ± 0.55 compared with control. These expression levels were similar to the calbindin-D28k content of DA cells at the extreme ends of the endogenous expression level distribution (**Fig. 2b**). Consistent with the correlation of P_v with endogenous calbindin-D28k levels, calbindin-D28k knockdown neurons exhibited an approximately fourfold greater single action potential exocytic response compared with control, whereas overexpression of calbindin-D28k reduced the single action potential responses approximately tenfold (**Fig. 3a**). Similarly, P_v increased substantially to 0.30 ± 0.04 in VTA calbindin-D28k knockdown neurons compared with control (0.11 ± 0.04, $P = 0.006$) and could be restored to near wild-type levels (0.14 ± 0.05, $P = 0.02$) by reintroduction of an shRNA-insensitive calbindin-D28k expression plasmid (**Fig. 3b**). In contrast knockdown of
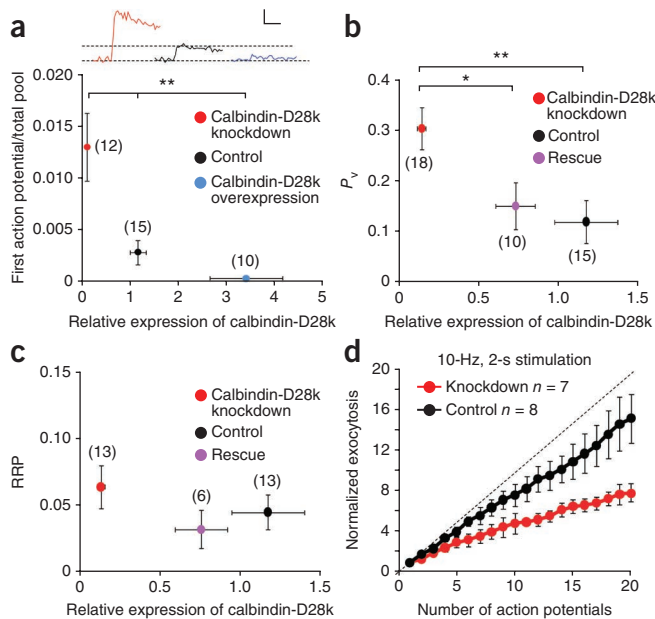
Figure 3 Calbindin-D28k knockdown in VTA DA neurons enhanced P_v and synaptic depression during action potential bursts. (**a**) Single action potential responses are significantly higher and lower in calbindin-D28k knockdown and overexpression neurons compared with control neurons (three-way ANOVA, $P < 0.0001$). Inset, representative one action potential responses for each condition. **$P < 0.01$. Scale bars represent 0.5% of total pool (see **Supplementary Fig. 1**), 50 ms. (**b,c**) P_v (**b**) and RRP (**c**) measured from control, calbindin-D28k knockdown and calbindin-D28k knockdown with rescue neurons plotted against relative expression of calbindin-D28k. *$P < 0.05$. (**d**) Amount of exocytosis relative to the first action potential response plotted against action potential number (straight line shows zero depression) in calbindin-D28k knockdown DA and control DA neurons.

calbindin-D28k in hippocampal neurons had no significant effect on P_v ($P = 0.22$; **Supplementary Fig. 2**). The increase in P_v by calbindin-D28k depletion was not the result of an increase in resting calcium levels (**Supplementary Fig. 5**). RRP sizes were not affected by loss of calbindin-D28k ($P = 0.32$, **Fig. 3c**); however, overexpressing calbindin-D28k frequently resulted in responses that appeared only after a long delay during the stimulus period with a much shallower slope in exocytosis, which prevented us from accurately extracting the RRP size and P_v (data not shown).

To examine the role of calbindin-D28k in a more physiological regime, we challenged control VTA DA neurons and calbindin-D28k knockdown VTA DA neurons with 20 action potentials at 10 Hz. Analysis of the cumulative vMAT-pHluorin signal normalized to first stimulus response amplitude showed that, in the absence of calbindin-D28k, exocytic responses of VTA neurons started to exhibit greater depression by the second or third action potential compared with controls. By the 20th stimulus, the net depression was ~2.5-fold greater in calbindin-D28k knockdown DA neurons than in control neurons (**Fig. 3d**). Similar results were obtained using 20-Hz stimulation (data not shown) and indicate that calbindin-D28k's ability to lower release probability allows them to more faithfully provide graded synaptic outputs during brief stimulus trains in VTA neurons.

The differential physiological control conveyed by calbindin-D28k in VTA versus SN neurons may also be important in pathological states such as Parkinson's disease, where the death of SN DA neurons is partially a result of cytosolic dopamine, oxidative stress, calcium toxicity and alpha-synuclein accumulation[11–13]. Neurons with no or low expression of calbindin-D28k were found to be more prone to death in disease development. Thus, calbindin-D28k–mediated calcium buffering was suggested as an important mechanism that provides protection to VTA neurons. In summary, our results identify an important control element that dictates exocytosis properties in VTA DA neurons, one that may serve as an important therapeutic target, independent of SN function.

METHODS

Methods and any associated references are available in the online version of the paper.

Note: Supplementary information is available in the online version of the paper.

AUTHOR CONTRIBUTIONS
P.-Y.P. and T.A.R. designed the experiments. P.-Y.P. performed the experiments. P.-Y.P. and T.A.R. analyzed the data and wrote the paper.

1. Grace, A.A. *Brain Res. Brain Res. Rev.* **31**, 330–341 (2000).
2. Hornykiewicz, O. *Neurology* **51**, S2–S9 (1998).
3. Cicchetti, F., Prensa, L., Wu, Y. & Parent, A. *Brain Res. Brain Res. Rev.* **34**, 80–101 (2000).
4. Sankaranarayanan, S. *Biophys. J.* **79**, 2199–2208 (2000).
5. Sankaranarayanan, S. & Ryan, T.A. *Nat. Cell Biol.* **2**, 197–204 (2000).
6. Onoa, B., Li, H., Gagnon-Bartsch, J.A., Elias, L.A. & Edwards, R.H. *J. Neurosci.* **30**, 7917–7927 (2010).
7. Liang, C.L., Sinton, C.M., Sonsalla, P.K. & German, D.C. *Neurodegeneration* **5**, 313–318 (1996).
8. Schwaller, B. *Cold Spring Harb. Perspect. Biol.* **2**, a004051 (2010).
9. Faas, G.C., Raghavachari, S., Lisman, J.E. & Mody, I. *Nat. Neurosci.* **14**, 301–304 (2011).
10. Ariel, P. & Ryan, T.A. *Front. Neural Circuits* **4**, 18 (2010).
11. Conway, K.A., Rochet, J.C., Bieganski, R.M. & Lansbury, P.T. Jr. *Science* **294**, 1346–1349 (2001).
12. Nedergaard, S., Flatman, J.A. & Engberg, I. *J. Physiol. (Lond.)* **466**, 727–747 (1993).
13. Sulzer, D. *Trends Neurosci.* **30**, 244–250 (2007).

ONLINE METHODS

Cell culture and immunocytochemistry. Dissociated midbrain neuronal cultures were prepared from postnatal day 0–1 Sprague-Dawley rat pups to provide either a mixture of VTA and SN or an enriched VTA DA neuron population. For the latter, we used a narrow section of midbrain adjacent to the midline, and for the mixed cultures (VTA and SN), we used a wider section extending beyond the midline (**Fig. 2c**). Dissected tissue was then prepared according to our previously published protocol[14], plated at a cell density of 130,000 cells per cm^2) and grown in the medium supplemented with GDNF (10 ng ml^{-1}). Hippocampal cultures were prepared as described previously[15]. Following experiments, all midbrain cultures were stained for the DA neuron–specific marker tyrosine hydroxylase. Neurons were fixed in PFA (containing 4% paraformaldehyde (wt/vol, EMS) and 4% sucrose, wt/vol) for 10 min, permeabilized in 0.2% Triton X-100 (vol/vol), and blocked with 5% BSA (wt/vol) for 40–60 min in 37 °C. Antibody to tyrosine hydroxylase (monoclonal, Calbiochem, cat# 657012) was diluted at 1:1,000 with 5% BSA and incubated with the cell at 37 °C for 1 h. After a 5 min wash with 1× PBS, cells where then incubated with a 1:1,000 dilution of Alexa Fluor 546 secondary antibody and antibody to GFP, Alexa Fluor 488 conjugate (Invitrogen, cat# A21311). For triple staining, mouse antibody to tyrosine hydroxylase (1:1,000, Calbiochem) with Alexa 633 (1: 500, Invitrogen, cat# A21052), chicken antibody to GFP (1:1,000, Abcam, cat# A10262) with Alexa 488 (1:1,000, Invitrogen, cat# A11039) and rabbit antibody to calbindin-D28k (1:1,000, Millipore, cat# AB1778) with Alexa 546 (1:1,000, Invitrogen, cat# A11035) were used. For comparison of calbindin-D28k immunoreactivity in VTA and hippocampal cultures, rabbit antibody to calbindin-D28k was taken from the same reaction tube, whereas mouse antibody to tyrosine hydroxylase was added for VTA culture and mouse antibody to MAP2 was added for hippocampal culture. Only midbrain neurons identified as tyrosine hydroxylase–positive were included in the analysis.

Constructs and transfection. A 29mer hairpin shRNA targeting calbindin-D28K was engineered into the pRS vector driven by U6 promoter using the following targeting sequence: 5′-AAGCAAACAAGACCGTGGATGATACGAAA-3′. The following primers were used to generate the rescue calbindin-D28k construct by using QuikChange II site-directed mutagenesis kit from Stratagene: 5′-GCT AGAGAAAGCCAACAAGACGGTGGACGATACGAAACTTG-3′ and 5′-CA AGTTTCGTATCGTCCACCGTCTTGTTGGCTTTCTCTAGC-3′ (underlined nucleotides indicate the incorporated mutations). pcDNA3.1–calbindin-D28k was a kind gift from A. Lee (University of Iowa). YC3.60 was obtained from A. Miyawaki (RIKEN). All constructs were sequenced before transfection. At 3 d *in vitro*, neurons were transfected using calcium phosphate and left for 10 d before all experiments were conducted. We added 10 ng ml^{-1} GDNF per dish after transfection to help the growth of dopaminergic neurons.

Optical setup and imaging. For live-cell imaging, cells were mounted on a custom-made laminar-flow stimulation chamber with constant perfusion (at a rate of ~0.2–0.3 ml min^{-1}) of a Tyrode's salt solution containing 119 mM NaCl, 2.5 mM KCl, 2 mM CaCl$_2$, 2 mM MgCl$_2$, 25 mM HEPES, 30 mM glucose, 10 μM 6-cyano-7-nitroquinoxaline-2,3-dione and 50 μM D,L-2-amino-5-phosphonovaleric acid, buffered to pH 7.4. All chemicals were purchased from Sigma except for bafilomycin (1 μM, Calbiochem) and Magnesium Green dye (MgGreen, 20 μM, Invitrogen). Temperature was clamped at 30.0 °C at the objective throughout the experiment. Field stimulations were delivered at 10 V cm^{-1} by A310 Accupulser and A385 stimulus isolator (World Precision Instruments). We used a 1-ms pulse to evoke single action potentials. Images were acquired using a highly sensitive, back-illuminated EM-CCD camera (iXon+ model # DU-897E-BV, Andor). A Zeiss Axiovert 200 microscope was modified for laser illumination. A solid-state diode-pumped 488-nm laser was shuttered using acoustic-optic tunable filters during non–data acquiring periods. pHluorin fluorescence excitation and collection was through a 40× 1.3 NA Fluar Zeiss objective using 515–560-nm emission filter and 510-nm dichroic filters (Chroma) and a 1.6× Optivar.

We used 10-Hz sampling for 10-Hz stimulations and 100-Hz sampling for 100-Hz stimulation (all the RRP measurements). For calcium imaging, 9 μM Fluo-5F or 20 μM MgGreen was loaded for 10 min and washed off for over 20 min in Tyrodes to reduce background. For calcium imaging with Fluo-5F, measurements were taken in Tyrodes containing 4 mM Ca^{2+}. We used 1,000-Hz sampling (0.74- or 0.72-ms exposure at frame transfer) at three pixel (equivalent to 0.75 μm) line scan to obtain enough temporal resolution for capturing the peak signal after EGTA-AM treatment. Normally, there are one to two responding boutons in the imaging field that colocalize with VAMP-mCherry. A test pulse (three action potentials at 3 Hz) was given before each experiment to make sure that single action potential elicited calcium signal does not saturate the dye. MgGreen was preferred for imaging Ca^{2+} entry at 100-Hz, 0.2-s stimulation because of its linearity over a large range of stimulation. Signals were sampled at 100 Hz (9.74- or 9.72-ms exposure at frame transfer) with 1-μs delay so that each data point corresponds to the accumulated [Ca^{2+}] at each stimulus. For resting calcium measurement with YC 3.60 (ref. 16), the indicator was excited by 430-nm laser with a single exciter (425/D40) and dichroic (at 460 nm). Two emitters (480/D40 and 550/D50) were switched manually by a filter slider. Yellow fluorescent protein and cyan fluorescent protein emissions were taken alternatively with 3-min spacing at 20-Hz, 0.5-s stimulations to monitor the viability and stability of the neuron. Immunofluorescence data was acquired using the identical optical system with exception that 532-nm and 633-nm laser sources were also used for illumination of alternate fluorescence channels.

Data analysis. Images were analyzed in ImageJ (http://rsb.info.nih.gov/ij/) using a custom-written plugin (http://rsb.info.nih.gov/ij/plugins/time-series.html). We placed circular ROIs (2 μm in diameter) on all varicosities that appear stable throughout all trials and responded to a maximal stimulus. To determine the RRP size, we used a sliding window method to find the plateau during accumulated pHluorin response[10]. A plateau representing the RRP size was identified as the largest data window in which the slope of the rise of the fluorescence (ΔF) versus action potential number was not significant. If there was more than one window of the same size where this condition was met, we used the one that came first during stimulation. To determine the RRP size, we averaged the ΔF values in the identified window. To measure single action potential response, 7–15 trials were given repetitively at about 30-s intervals. By averaging, we were able to obtain a pHluorin response (for all the stable boutons in the field) with sufficient signal-to-noise to identify ΔF, which is over 2× of the baseline noise (s.d.). We considered a cell to have no response when ΔF was under 2× of the baseline noise of the averaged response and assigned it to be $\Delta F = 0$, and hence, $P_v = 0$. Calbindin-D28k staining was measured at the cell body and corrected by local background. Fluorescence intensities measurements for calbindin-D28k staining were corrected for a small (13.8%) bleed through from the 633-nm channel used for tyrosine hydroxylase staining. In **Figure 2a,b**, we took the immunoreactivity at the cell body for each tyrosine hydroxylase–positive cell after background subtraction and bleed through correction, and normalized it to the average value (taken as 1) from the whole sample obtained using the same calculation. In **Figure 2d** and **Supplementary Figure 4**, calbindin-D28k levels were calculated in the same way except that they were then normalized to the average calbindin-D28k expression in VTA DA neurons. In figures in which retrospective immunostaining was carried out to determine the relative expression of calbindin-D28k of the tested cell, we randomly sampled 4~8 tyrosine hydroxylase–positive neurons in the same and nearby fields and took that to represent the whole sample. All data are presented as mean ± s.e.m. Student t test (two tail) was used for statistical tests unless otherwise noted.

14. Mani, M. & Ryan, T.A. *Front. Neural Circuits* **3**, 3 (2009).
15. Kim, S.H. & Ryan, T.A. *Neuron* **67**, 797–809 (2010).
16. Nagai, T., Yamada, S., Tominaga, T., Ichikawa, M. & Miyawaki, A. *Proc. Natl. Acad. Sci. USA* **101**, 10554–10559 (2004).